한국동력기계공학회지 제17권 제5호 pp. 44-51 2013년 10월 (ISSN 1226-7813)
Journal of the Korean Society for Power System Engineering, Vol. 17, No. 5, pp. 44-51, October 2013
Research paper

Barrier-Transition Cooling in LED

Jedo Kim†

(received 31 August 2013, revised 8 October 2013, accepted 8 October 2013)

Abstract : This paper proposes and analyzes recycling of optical phonons emitted by nonradiative decay, which is a major thermal management concern for high-power light emitting diodes (LED), by introducing an integrated, heterogeneous barrier cooling layer. The cooling is proportional to the number of phonons absorbed per electron overcoming the potential barrier, while the multi-phonon absorption rate is inversely proportional to this number. We address the theoretical treatment of photon-electron-phonon interaction/transport kinetics for optimal number of phonons (i.e., barrier height). We consider a GaN/InGaN LED with a metal/AlGaAs/GaAs/metal potential barrier and discuss the energy conversion rates. We find that significant amount of heat can be recycled by the barrier transition cooling layer.

Key Words : Recycling, Phonon, Cooling, LED, Barrier, Transition, Heat

— Nomenclature —

J_e : Electrical current [A]
$\dot{S}_{p-e,C}$: Transition cooling rate [W]
$\dot{S}_{e-p}$: Non-radiative emission [W]
$\dot{S}_{e-ph}$: Radiative emission [W]
Q_{e-p} : Net phonon produced [W]
A_{e-ph} : Radiative decay constant [cm3/s]
n_e : Carrier concentration [cm^{-1}]
A_{SHR} : Shockly-Read-Hall coefficient [s^{-1}]
A_{Auger} : Auger coefficient [cm^6/s]
m : Atomic mass [kg/mole]
u : Acoustic velocity [m/s]
f^o : Distribution function
E_e : Electron energy [eV]
N_p : Number of absorbed phonon
$E_{e,c}$: Electron energy over conduction edge

Greek Symbols

$\Delta\varphi_b$: Potential barrier [eV]
$\Delta\varphi_e$: Electrical potential [V]
$\dot{\gamma}_{ph}$: Radiative transition rate [s^{-1}]
ρ : Density [kg/m^3]
ω : Frequency [rad/s]
γ_G : Gruneisen parameter
Γ : Force constant [N/m]
φ'_{e-p} : Optical deformation potential [eV/m]

Subscripts

p : Phonon
p,A : Acoustic phonon
p,O : Optical phonon
AA : Anion
CC : Cation

† Jedo Kim(corresponding author) : Department of Mechanical Engineering, Pukong National University.
E-mail : jedokim@pknu.ac.kr, Tel : 051-629-6131

1. Introduction

LED lighting currently has up to 35% plug-in-efficiency (3-fold larger than incandescent lighting)[1], however its concentrated heat loss requires elaborate heat sinks[2]. In incandescent lamp the heat loss is due to the nonvisibile photon emission, and this radiation is spread over the large surface area of the lamp[3]. However, in LEDs the loss is through phonon emission (by nonradiative decay and other processes) which is transported through the solid structure (chip and its substrate)[4]. Moreover, the current LED thermal-damage threshold is about 100 ℃, thus making its thermal management challenging[1]. Heterogenous thermionic cooling is ballistic transport of nonequilibrium electrons over a potential barrier created by a heterogenous layer with the energy supplied by absorption of phonon [5~8], A successful implementation of AlGaAs/GaAs multiphonon-absorption barrier transition has been experimentally demonstrated with increase in the open-circuit voltage in solar cells[9]. Various theoretical models and predictions have shown that its coefficient of performance is much larger than that of the thermoelectric cooling[7),10~13]. Such models focus mainly on the electron transport across potential barriers created by the work function differences and current density j_e predicted by the Richardson equation which does not address the electron-phonon kinetics at the atomic level (done for various photonic systems [14~16]). In this paper we consider recycling a part of the emitted phonons through the use of a barrier transition cooling (BTC) layer (or BTCL) at the LED chip level.

2. Theoretical Analysis

We address various energy conversion and transport processes and rates (including multiphonon absorption) in BTCL-LED, identify the bottleneck process. Then, we tune the BTCL barrier height for maximum energy conversion efficiency, BTCL, not requiring a separate circuit, suits well in a series arrangement in the LED chip, as shown in Fig. 1(a). We consider a heterogenous LED chip with an adjacent metal/barrier/metal BTCL. External potential drives the electrons over the potential barrier $\Delta\varphi_b$ (by absorption of phonons) created by a heterogeneous layer. Then the electrons are injected into the LED chip for radiative transition and nonradiative decays. The phonon generated by the nonradiative transition in the LED chip is transferred by various phonon transport mechanism such as optical/acoustic phonon transmission and phonon up/down transport mechanism such as optical/acoustic phonon transmission and phonon up/down conversion at the interface. The conceptual energy diagram and energy conversion is shown in Fig. 1(b) and the energy flow diagram of input power $J_e\Delta\varphi_e$ (product of current and electric potential across LED), barrier transition cooling $\dot{S}_{p-e,C}$, nonradiative emission $\dot{S}_{e-p}$, radiative emission $\dot{S}_{e-ph}$, and net phonon produced Q_{e-p} are shown in Fig. 1(c).

By recycling phonons emitted by nonradiative emission, larger electrical energy is not necessary to drive the cooling system, as long as the phonon absorption rate is not the bottleneck process. We now analyze these related interactions to identify the bottleneck processes while making some reasonable assumptions. The proposed BTCL-LED is addressed considering the interplays among the three energy carriers (photons, phonon, and electron) and their interaction rates based on the Fermi golden rule.

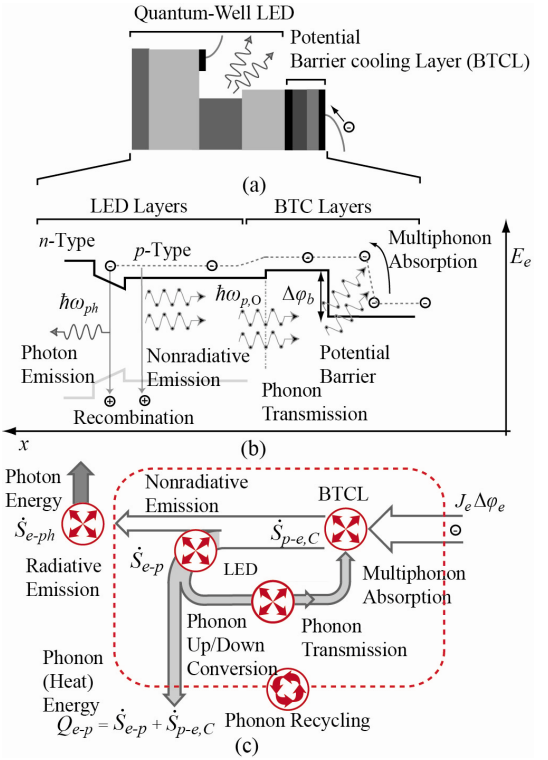

Fig. 1 (a) Integrated LED layer and metal/barrier /metal BTCL. (b) The conduction electron energy diagram and related carrier transitions. (c) The energy flow diagram of such BTCL integrated LED chip. Although the available chip-level simulation analysis[17] can be applied for detailed performance, here we focus on the carrier transitions and the kinetics of carrier interactions in order to identify the multiphonon absorption bottlenecks and phonon recycling limits. The relevant carrier transitions in LED and BTCL are shown in Figs. 2(a) to (d). Figure 2(a) shows the radiative transition and the nonradiative transitions in LEDs producing photons and phonons respectively. Figure 2(b) shows the phonon transmission processes between LED and BTCL, i.e., the optical and acoustic phonon transmissions and the optical phonon decay. Figure 2(c) shows the phonon-phonon upconversion and Fig. 2(d) electron-phonon transition processes in BTCL.

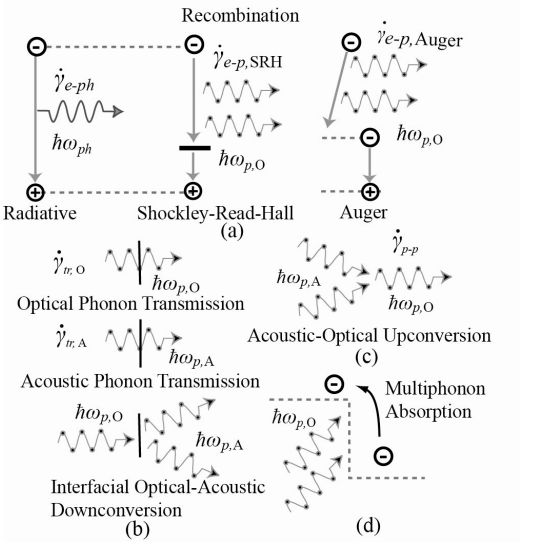

Fig. 2 Detailed carrier transitions are shown for (a) radiative and nonradiative transitions in LED, (b) phonon transmission in LED/BTCL boundary, and (c) phonon upconversion (d) multiphonon absorption in BTCL.

We only consider the optical phonon absorption, because this is found to be an order of magnitude larger than acoustic phonon absorption rate[18] (which is extremely low multiphonon absorption due to relatively low energies). The radiative transition rate $\dot{\gamma}_{ph}$ in LED is linearly dependent on the carrier concentration and is simply given by[19]

$$\dot{\gamma}_{e-ph} = A_{e-ph} n_e \tag{1}$$

where A_{e-ph} is the radiative decay constant and n_e is the carrier concentration. Note that we use units of s^{-1} for transition rates.

The dominant nonradiative decays are the Shockley-Read-Hall (SHR) and Auger recombination. The SHR recombination is due direct multiphonon decay at the defect sites, while the Auger recombination is due to transfer of energy to a conduction electron followed by a multiphonon decay. These nonradiative recombination are

commonly presented with simple expressions (e.g., for GaN[19]). The total nonradiative transition rate $\dot{\gamma}_{e-p}$ depend on the carrier concentration (SHR is given as a constant coefficient, while the Auger has a quadratic dependence) as

$$\dot{\gamma}_{e-p} = A_{SHR} + A_{auger} n_e^2 \tag{2}$$

where A_{SHR} and A_{Auger} are the Shockly-Read_Hall and Auger recombination coefficients respectively. The phonon frequencies generated by these nonradiative transitions depend on the highest available phonon frequency in the lattice and decay to the lower frequencies via phonon-phonon interaction processes.

The phonon generated by the nonradiative transition in LED is transmitted to the BTCL by various phonon-phonon transitions and transmission processes. Significant optical phonon population is available in GaN, due to the large optical phonon life-times {when cation and anion mass ratio m_C/m_A > 4, LO (longitudinal optical) → 2TA (transverse acoustic) or 2LA (longitudinal acoustic) decay channels are unavailable and the dominate decay channel is found to be LO → {LO + LA(TA)}. These optical phonon modes is first transmitted to the metal layer which acts as a contact between the LED and BTCL. Since for metals such as Al, there are no optical branches and the optical phonon modes must be downconverted in order to propagate within. The down conversion rate in the metal layer can be calculated by three phonon interaction model given as

$$\dot{\gamma}_{p-p} = \frac{\hbar}{8\pi\rho^3}\frac{|M_{p-p}|^2 R}{u_{p,A}^7 u_{p,O}^2}\omega_{p,A}^2\omega_{p,O}^3 \times \left[f_p^o(\omega_{p,A})+1\right]\left[f_p^o(\omega_{p,A})+1\right]\left[f_p^o(\omega_{p,O})\right]$$
$$|M_{p-p}|^2 = 4\rho^2\gamma_G^2 u_{p,A}^2 u_{p,O}^2 \ , \ R = \frac{2}{3^{1/2}}\frac{\Gamma_{AA}-\Gamma_{CC}}{\Gamma_{AA}+\Gamma_{CC}} \tag{3}$$

where ρ is the density, $u_{p,A}$ and $u_{p,O}$ are the acoustic and optical phonon velocities respectively, $\omega_{p,A}$ and $\omega_{p,O}$ are the acoustic and optical phonon frequencies respectively, f_p^o is the phonon distribution function, γ_G is the Grüneisen parameter, and Γ_{AA} and Γ_{CC} are the force constants which can be estimated by material metrics[14),20)]. We have used the DebyeEinstiein phonon density of states model and assumed that the two acoustic phonons are identical.

Acoustic phonon transmission rate can be estimated by dividing transmission length (L) by acoustic velocity and the transmission coefficient is predicted by diffuse mismatch model(DMM) using the difference in the mode velocities across the interface. Considering transverse acoustic waves have velocities of 6420 m/s, 3960 m/s and 2800 m/s respectively in aluminum, zinc-blend GaN and GaAs in [111] direction (we take a conservative approach and take the smaller values) then the inverse of the acoustic mode propagation time through Al, GaN and GaAs can be estimated to be of the order of $10^{10}\,\mathrm{s}^{-1}$ up to $1\mu\mathrm{m}$ in combined length which is extremely fast. Although we our predicted DMM-based transmission coefficient are 0.80 for GaN/Al and 0.55 for Al/GaAs interfaces, the availability of the acoustic modes in the BTCL layer not expected to limit the kinetics of the system due to much higher transition rate compared to the electron transition rates.

Acoustic modes available in the BTCL can be upconverted to form higher energy phonons to be used in the multiphonon absorption process across the potential barrier and this rate can be also calculated by three phonon interaction model given as

$$\dot{\gamma}_{p-p} = \frac{\hbar}{8\pi\rho^3}\frac{|M_{p-p}|^2 R}{u_{p,A}^7 u_{p,O}^2}\omega_{p,A}^2\omega_{p,O}^3 \times f_p^o(\omega_{p,A}) f_p^o(\omega_{p,A})\left[f_p^o(\omega_{p,O})+1\right] \tag{4}$$

where the distribution functions are modified for annihilation of two acoustic phonons and creation of one optical phonon.

We formulate the electron transition over the potential barrier $\triangle\varphi_b$ as an optical phonon absorption process in the presence of a bias voltage. The relation for single optical phonon absorption rate in semiconductors is derived using the Fermi golden rule and is [18)]

$$\dot{\gamma}_{p-e} = \frac{\varphi'^2_{e-p} m_{e,e}^{3/2} E_e^{1/2} f_p^o(E_p)}{2^{1/2}\pi\hbar^3\rho\omega_{p,O}} \tag{5}$$

where φ'_{e-p} is the optical phonon deformation potential, $m_{e,e}$ is the reduced electron mass, and E_e is the electron energy. We have used the parabolic band assumption for the electronic density of states near the bandedge.

Here, in order to predict the performance of the integrated BTCL/LED system, we take various properties from a sample LED found in ref 19). We assume temperature independence of the properties since we expect that the BTCL will limit any significant temperature increase. Also, all the temperature dependance is taken care of by the distribution function when we calculate the rates of the processes.

Table 1 Various transition rates (s^{-1}) for sample LED and BTCL using properties found in ref. 19). $n_e = 5\times10^{18} cm^{-3}$, $A = 10^{-6} m^2$ and T = 323 K are used throughout. The current density can be found by $j_e/e_c = \dot{\gamma}_{i-j}/A$(number of electrons per unit area per second), where e_c is electron charge.

$\dot{\gamma}_{e-ph}$ [a]	$\dot{\gamma}_{e-p,SHR}$ [b]	$\dot{\gamma}_{e-p,Auger}$ [c]	$\dot{\gamma}_{p-p}$ [d]	$\dot{\gamma}_{p-e}$ [e]
5.5×10^7	2.4×10^7	3.5×10^7	1.5×10^8	6.0×10^{11}

a. $A_{e-ph} = 1.1\times10^{-11}\,\mathrm{cm^3 s^{-1}}$ $\gamma_G = 0.8$

b. $A_{SHR} = 2.4\times10^7\,\mathrm{s^{-1}}$ $R = 0.128$

c. $A_{Auger} = 1.4\times10^{-30}\,\mathrm{cm^6 s^{-1}}$

d. $\rho = 5317\,\mathrm{kg/m^3}$
$u_{p,A} = 2800\,\mathrm{m/s}$
$\omega_{p,O} = 8.6\,\mathrm{THz/s}$
$\omega_{p,A} = 4.3\,\mathrm{THz/s}$

e. $\varphi'_{e-p} = 9.0\,\mathrm{eV/Å}$
$m_{e,e} = 0.0819 m_e$
$E_e = 0.05\,\mathrm{eV}$
$\hbar\omega_{p,O} = 0.035\,\mathrm{eV}$

From Table 1, the single-phonon absorption rate is much faster than other processes. This suggests multiphonon absorption can be accommodated in the TCL, i.e., we can use a barrier height exceeding the available single phonon energy. We use the commonly used exponential dependence (of the phonon distribution function) for the multiphonon transition processes given as

$$\dot{\gamma}_{p-e,C} = \dot{\gamma}_{p-e} f_p^{oN_p - 1} \tag{6}$$

where N_p is the number of absorbed phonons. The variation of the multiphonon transition rate with respect to N_p is shown in Fig. 3 along with the LED total transition rate $\dot{\gamma}_T$.

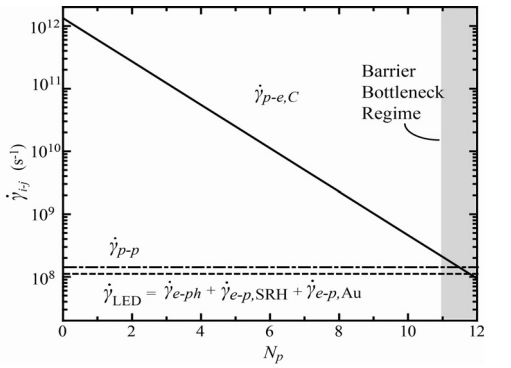

Fig. 3 Variation of multiphonon transition rate with respect to the number of phonons absorbed.

3. Discussion

From the results, the multiphonon transition rate becomes the bottle neck process at $N_p = 11$ for $\hbar\omega_{p,O}$= 0.035 eV. So, when the barrier height exceeds approximately 0.4 eV, the electron transition over the potential barrier becomes the limiting process, thus reducing the electron injection into the LED layer. This will then significantly reduce the LED performance and is not desirable.

We now calculate the performance of LED with a BTCL by using the transition rates under constant current assumption. When the BTCL is added to the LED, the barrier acts as an extra resistance and has an adverse effect on the current which produces extra phonons (Joule heating). This adverse effect will reduce the total radiative transition rate by the second term given below

$$\dot{\gamma}_{e-ph} - e^{-(E_{e,c}-N_p\hbar\omega_p)/k_BT}\dot{\gamma}_T \tag{7}$$

where $E_{e,c}$ is the electron energy over the conduction bandedge at the bottom of the barrier potential and results in an additional nonradiative emission given by the second term below

$$\dot{\gamma}_{e-ph} + e^{-(E_{e,c}-N_p\hbar\omega_p)/k_BT}\dot{\gamma}_T \tag{8}$$

here we take $E_{e,c}$ as $0.45eV$ to ensure a constant current up to the barrier bottleneck (i.e., $N_p = 11$). The energy conversion rate is given by $\dot{S}_{i-j} = \hbar\omega_{i,j} n_e V \dot{\gamma}_{i-j}$ where V is the volume. We define the overall quantum efficiency as $\eta_{e-ph} = \dot{S}_{e-ph}/(\dot{S}_{e-ph} + \dot{S}_{e-p} + \dot{S}_{p-e,C})$, which is the ratio of the photon emission rate to the total input power (including the power required for cooling). The calculated results are shown in Fig. 4 for $V = 10^{-12} m^3$ the sample LED produces 1.5 and 1.4 W of phonon and photon energy, respectively. When the BTCL of 100 nm is added (shown with $N_p > 0$), the adverse effect on the current increases the phonon emission and decreases the photon emission as the barrier height is increased. Therefore, it is predicted that barrier height over 0.35 eV will emit significant number of extra phonons which will destabilize the system. Note that BTCL thickness should be large enough to avoid any quantum well effect. The barrier transition cooling rate $\dot{S}_{p-e,C}$ increases with N_p due to higher energy absorbed per transition, while the kinetics is limited by LED total transition (i.e., $\dot{\gamma}_{e-ph} + \dot{\gamma}_{e-p,SRH} + \dot{\gamma}_{e-p,Auger}$). Above $N_p = 11$, performance is limited by the barrier bottleneck in Fig. 3. We find that η_{e-p} peaks at $N_p = 8$ which corresponds to a barrier height of 0.288 eV which is a 17% improvement over the LED with no such BTCL. The results in Fig. 4 also show that the quantum efficiency slightly increases as non-radiative decay is limited as the multi-phonon transition rate increases. However, when the barrier height becomes too large (above Np = 9), the quantum efficiency drops sharply due to significant non-radiative decay caused by back flow of electrons because of the high energy barrier.

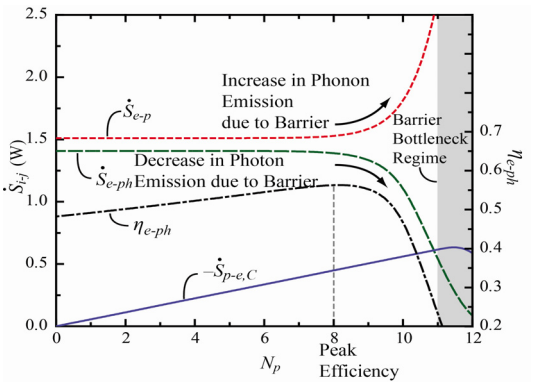

Fig 4. Variation of the energy conversion rate with respect to the number of phonons required to overcome the potential barrier. The overall quantum efficiency is also shown.

This recycles up to 30% of heat (phonon) generated by the nonradiative decay reducing required heat removal load in operating LED (then requiring a smaller heat sink).

5. Conclusions

Note that the above calculations are for the cooling rate $\dot{S}_{p-e,C}$ based on the equilibrium phonon population at T = 323 K. However, when phonon transport path short (as is here) and for materials (such as GaN and InN) containing significant mass miss match (between cations and anions), the multiphonon transition rate is influenced by nonequilibrium optical phonons due to long lifetime of optical phonon modes. Such nonequilibrium contribution also encountered and discussed in other photonic systems[15], but is rather difficult to quantify the LED system.

Acknowledgement

This work was supported by a Research Grant of Pukyong National University (2013).

References

1. E. F. Schubert, 2006, "Light-Emitting Diodes" (Cambridge University Press, 2nd ed.)
2. M. Arik and A. Setlur, 2009, "Environmental and economical impact of LED lighting systems and effect of thermal management" International Journal of Energy Research, Vol. 34, pp. 1195-1202.
3. M. Kaviany, 2002, "Principles of Heat Transfer" Wiley, Cambridge.
4. G. Held, 2008, "Introduction to Light Emitting Diode Technology and Applications" (Auerbach Publications, Boca Raton, 2008).
5. G. D. Mahan and L. M. Woods, 1998, "Multilayer Thermionic Refrigeration" Physical Review Letters, Vol. 80, pp. 4016-4019.
6. G. D. Mahan, L. M. Woods, and M. Bartkowiak, 1998, "Multilayer thermionic refrigerator and generator" Journal of Applied Physics, Vol. 83, pp. 4683-4690.
7. A. Shakouri and J. E. Bowers, 1997, "Heterostructure integrated thermionic coolers" Applied. Physics Letters, Vol. 9, pp. 1234-1237.
8. A. Mal'shukov and K. Chao, 2001, "Opto-Thermionic Refrigeration in Semiconductor Heterostructures", Physical Review Letters, Vol. 86, pp. 5570-5573.
9. F. W. Ragay, E. W. M. Ruigrok, and J. H. Wolter, 1994, "GaAs-AlGaAs heterojunction solar cells with increased open-circuit voltage" IEEE Photovoltaic Specialists Conference 2, pp. 1934-1940.
10. B. C. Lough, S. P. Lee, R. A. Lewis, and C. Zhang, 2001, "Numerical calculation of thermionic cooling efficiency in a double-barrier semiconductor heterostructure" Physica E 11, pp. 287-291.
11. P. Han, K. Jin, Y. Zhou, X. Wang, Z. Ma, S. Ren, A. Mal'shukov and K. A. Chao, 2006, "Analysis of optothermionic refrigeration based on semiconductor heterojunction", Journal of Applied Physics, Vol. 99, pp. 074504-074509.
12. S. Yen and K. Lee, 2010, "Analysis of heterostructures for electroluminescent refrigeration and light emitting without heat generation", Journal of Applied Physics, Vol. 107, pp. 054513-054522.
13. P. Han, K. Jin, Y. Zhou, H. Lu, and G. Yang, 2007, "Numerical designing of semiconductor structure for optothermionic refrigeration", Journal of Applied Physics, Vol. 101, pp. 014506-014510.
14. J. Kim, A. Kapoor, and M. Kaviany, 2008,

"Material Metrics for laser cooling of solids" Physical Review B, Vol. 77, 115127-115142.
15. J. Kim, and M. Kaviany, 2009, Phonon Recycling in Ion-doped Lasers", Applied Physics Letters, Vol. 95, pp. 074103-074106.
16. J. Kim, and M. Kaviany, 2010, "Phonon Coupling Enhanced Absorption of Alloyed Amorphous Silicon for Solar Photovoltaics", Physical Review B, Vol. 82, pp. 134205-134211.
17. J. Piprek, 2007, "Nitride Semiconductor Devices: Principles and Simulation" (Wiley-VCH, Weinheim).
18. J. Singh, 2003, "Electronic and Optoelectronic Properties of Semiconductor Blue Lasers and Light Emitting Diodes" (Cambridge University Press.)
19. S. Nakamura and S. Chichibu, 2000, "Introduction to Nitride Semiconductor Blue Lasers and Light Emitting Diodes" (CRC Press, New York, 2000).
20. G. P. Srivastava, 1990, "The Physics of Phononons"(Taylor & Francis, NewYork).